

# A Dynamic Grouping Strategy for Beyond Diagonal Reconfigurable Intelligent Surfaces with Hybrid Transmitting and Reflecting Mode

Hongyu Li, *Student Member, IEEE*, Shanpu Shen, *Member, IEEE*, and Bruno Clerckx, *Fellow, IEEE*

**Abstract**—Beyond diagonal reconfigurable intelligent surface (BD-RIS) is a novel branch of RIS which breaks through the limitation of traditional RIS with diagonal scattering matrices. However, the existing research focuses on BD-RIS with fixed architectures regardless of channel state information (CSI), which limit the achievable performance of BD-RIS. To solve this issue, in this paper, we propose a novel dynamically group-connected BD-RIS based on a dynamic grouping strategy. Specifically, RIS antennas are dynamically divided into several subsets adapting to the CSI, yielding a permuted block-diagonal scattering matrix. To verify the effectiveness of the proposed dynamically group-connected BD-RIS, we propose an efficient algorithm to optimize the BD-RIS with dynamic grouping for a BD-RIS-assisted multi-user multiple-input single-output system. Simulation results show that the proposed dynamically group-connected architecture outperforms fixed group-connected architectures.

**Index Terms**—Beyond diagonal reconfigurable intelligent surface (BD-RIS), dynamic grouping.

## I. INTRODUCTION

Reconfigurable intelligent surface (RIS) has emerged as a revolutionary technique enabling spectrum, cost, and energy efficient communications [1], [2]. However, most existing works focus on a simple RIS architecture, where each RIS element is connected to a load disconnected from the other elements, yielding mathematically a diagonal phase shift matrix. This architecture enables the phase shift control of the incident waves and can only support the signal reflection, which limits the beam control accuracy and coverage of RIS.

To break through the limitation of traditional RIS, a novel branch namely beyond diagonal RIS (BD-RIS) as illustrated in Fig. 1, has been recently proposed and investigated. The BD-RIS relies on different circuit topologies of antenna ports and thus has scattering matrices beyond diagonal matrices. Specifically, modeling and architecture design of RIS and microwave theory was first bridged in [3]. The authors proposed more general group- and fully-connected architectures, leading to block-diagonal scattering matrices and enabling more flexible dual phase shift and amplitude control of the impinging waves. Furthermore, group/fully-connected RIS with discrete-value impedance networks was investigated in [4]. Another

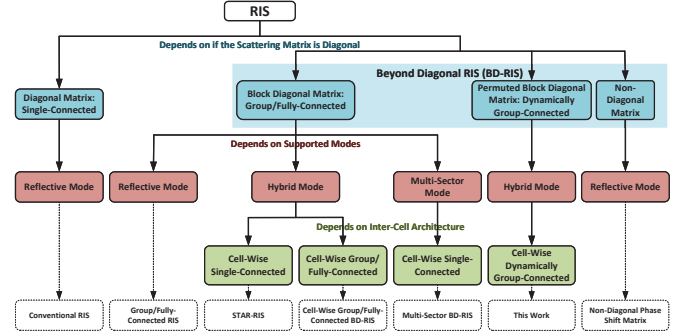


Fig. 1. RIS classification tree.

novel architecture with a non-diagonal phase shift matrix was proposed in [5]. However, the BD-RIS models proposed in [3], [4], [5] are restricted to the reflective mode, that is signals can only be reflected to one side of the surface, resulting a “waste” of space. To make full use of the space and realize a full-dimensional coverage, simultaneously transmitting and reflecting RIS (STAR-RIS) supporting the hybrid mode has been proposed recently as an important extension of RIS [6], [7]. To go deep into the essence of STAR-RIS, a general BD-RIS model unifying modes and architectures has been established in [8], showing that STAR-RIS is essentially a particular instance of group-connected architecture when group size is equal to 2. More general cell-wise group/fully-connected architectures for BD-RIS under the hybrid mode were also proposed. The work in [8] was further extended to a multi-sector mode, which can not only achieve full-space coverage, but also provide significant performance gain [9].

The limitation of the proposed BD-RIS architectures in [3], [8], [9] is that they are restricted to fixed grouping strategies, where all RIS antennas are uniformly partitioned and adjacently grouped regardless of channel state information (CSI). However, exploring different grouping strategies of BD-RIS still remains an open problem. To solve this issue, in this paper, we propose a dynamically group-connected BD-RIS model, which is a novel branch of BD-RIS as shown in Fig. 1. Specifically, the proposed dynamically group-connected BD-RIS model is based on a dynamic grouping strategy, whose main idea is to dynamically partition RIS antennas into multiple groups with variable group sizes adapting to CSI. The contributions of this paper are summarized as follows.

*First*, we model and analyze the proposed dynamically group-connected BD-RIS. *Second*, we apply the dynamical

Manuscript received; (*Corresponding author: Shanpu Shen*).

H. Li and B. Clerckx are with the Department of Electrical and Electronic Engineering, Imperial College London, London SW7 2AZ, U.K. (email: {c.li21,b.clerckx}@imperial.ac.uk).

S. Shen is with the Department of Electronic and Computer Engineering, The Hong Kong University of Science and Technology, Clear Water Bay, Kowloon, Hong Kong (email: sshenaa@connect.ust.hk).

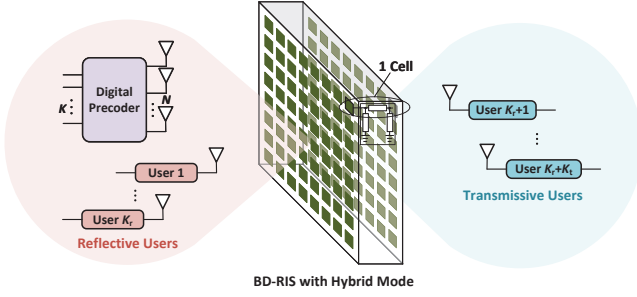


Fig. 2. Diagram of BD-RIS supporting the hybrid mode.

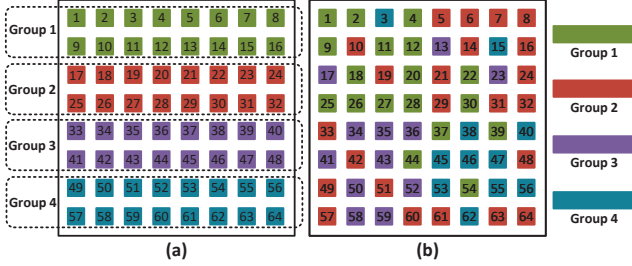


Fig. 3. Two grouping strategies: (a) fixed grouping; (b) dynamic grouping.

cally group-connected BD-RIS in a multi-user multiple-input multiple-output (MU-MISO) system and propose an efficient algorithm to optimize the BD-RIS with the dynamic grouping strategy. *Third*, we provide simulation results to evaluate the performance enhancement of the proposed dynamically group-connected BD-RIS compared to fixed group-connected cases.

## II. DYNAMICALLY GROUP-CONNECTED BD-RIS MODEL

In this section, we first briefly review the concept and mathematical model of cell-wise group-connected (CW-GC) BD-RIS with the hybrid mode proposed in [8]. Then we introduce the concept and mathematical model of cell-wise dynamically group-connected (CW-DGC) BD-RIS.

### A. CW-GC BD-RIS

As illustrated in [8] and also in Fig. 1, the hybrid mode is essentially based on the group-connected reconfigurable impedance network. More specifically, in the hybrid mode, each two antenna ports are connected to each other, thereby constructing one “cell” as illustrated in Fig. 2. Within each cell, two antennas are back to back placed such that each antenna covers half space. When different cells are connected to each other, the BD-RIS has a CW-GC architecture. Define  $\Phi_r \in \mathbb{C}^{M \times M}$  and  $\Phi_t \in \mathbb{C}^{M \times M}$  as scattering matrices in charge of users from both sides of the hybrid BD-RIS, which are constrained by [8]

$$\Phi_r^H \Phi_r + \Phi_t^H \Phi_t = \mathbf{I}_M. \quad (1)$$

We consider a simple CW-GC case with a fixed architecture regardless of CSI in [8] and assume that  $M$  cells of the hybrid BD-RIS is uniformly divided into  $G$  subsets indexed by  $\mathcal{G} = \{1, \dots, G\}$ , each of which groups a smaller number of adjacent RIS cells, i.e.,  $\bar{M} = M/G$ , to form a fully-connected network. For ease of understanding, we provide a

simple example with 64 cells and 4 groups in Fig. 3(a). Define  $G$  subsets

$$\mathcal{G}_g = \{(g-1)\bar{M} + 1, \dots, g\bar{M}\}, \forall g \in \mathcal{G}, \quad (2)$$

each of which denotes the set of cell indexes for group  $g$ ,  $\forall g \in \mathcal{G}_g$ . Then for CW-GC BD-RIS, constraint (1) of  $\Phi_r$  and  $\Phi_t$  can be rewritten as

$$\Phi_r = \text{blkdiag}(\Phi_{r,\mathcal{G}_1}, \dots, \Phi_{r,\mathcal{G}_G}), \quad (3a)$$

$$\Phi_t = \text{blkdiag}(\Phi_{t,\mathcal{G}_1}, \dots, \Phi_{t,\mathcal{G}_G}), \quad (3b)$$

$$\Phi_{r,\mathcal{G}_g}^H \Phi_{t,\mathcal{G}_g} + \Phi_{t,\mathcal{G}_g}^H \Phi_{r,\mathcal{G}_g} = \mathbf{I}_M, \forall g \in \mathcal{G}, \quad (3c)$$

where  $\Phi_{i,\mathcal{G}_g} \in \mathbb{C}^{\bar{M} \times \bar{M}}, \forall g \in \mathcal{G}$ .

### B. CW-DGC BD-RIS

We propose a novel architecture to improve the performance of CW-GC BD-RIS by adapting the grouping strategy to channel environments, which is referred to as the CW-DGC architecture<sup>1</sup>. To facilitate understanding, we illustrate the dynamic grouping strategy when the BD-RIS has 64 cells and 4 groups in Fig. 3(b). The word “dynamic” we use here is mainly embodied in two aspects: *i*) The size of each group can be different; *ii*) the positions/indexes of cells in the same group are not restricted to adjacent ones. To model this dynamic grouping strategy, we first present the following definition.

**Definition 1.** Define  $G$  subsets  $\mathcal{D}_1, \dots, \mathcal{D}_G$  which store indexes of RIS cells for each group. These subsets satisfy the following constraints:

$$\mathcal{D}_p \cap \mathcal{D}_q = \emptyset, \forall p \neq q, p, q \in \mathcal{G}, \quad (4a)$$

$$\mathcal{D}_g \neq \emptyset, \forall g \in \mathcal{G}, \quad (4b)$$

$$\bigcup_{g=1}^G \mathcal{D}_g = \mathcal{M}, \quad (4c)$$

which indicate *i*) that each RIS cell can only be mapped into one group, *ii*) that each group contains at least one cell, and *iii*) that there is no overlap among different groups.

Based on Definition 1, we have the following corollary.

**Corollary 1.** The scattering matrix of the CW-DGC BD-RIS should satisfy<sup>2</sup>

$$[\Phi_t]_{m,n} = 0, \forall m \in \mathcal{D}_p, \forall n \in \mathcal{D}_q, \forall p \neq q, p, q \in \mathcal{G}, \quad (5a)$$

$$[\Phi_r]_{m,n} = 0, \forall m \in \mathcal{D}_p, \forall n \in \mathcal{D}_q, \forall p \neq q, p, q \in \mathcal{G}, \quad (5b)$$

$$\Phi_{t,\mathcal{D}_g}^H \Phi_{t,\mathcal{D}_g} + \Phi_{r,\mathcal{D}_g}^H \Phi_{r,\mathcal{D}_g} = \mathbf{I}_{|\mathcal{D}_g|}, \forall g \in \mathcal{G}, \quad (5c)$$

where  $\Phi_{t/r,\mathcal{D}_g}$  is a sub-matrix of  $\Phi_{t/r}$  which selects rows and columns of  $\Phi_{t/r}$  according to indexes in the set  $\mathcal{D}_g, \forall g \in \mathcal{G}$ .

**Remark 1.** Comparing constraints (3) to (5), we have two observations. *i*) The scattering matrix of the CW-DGC BD-RIS is essentially a permuted block-diagonal matrix; *ii*) the

<sup>1</sup>The dynamically group-connected architecture refers to the inter-cell architecture, while the antenna ports within the same cell are always connected to each other regardless of CSI to support the hybrid mode.

<sup>2</sup>In this work we consider the hybrid mode of CW-DGC BD-RIS for simplicity. However, the proposed CW-DGC architecture can also support multi-sector mode and the illustrated model can be easily extended to the multi-sector case.

CW-GC case where  $\Phi_r$  and  $\Phi_t$  are block-diagonal matrices is a special instance of the CW-DGC case.

In the following section, we will apply the CW-DGC BD-RIS in a MU-MISO system and propose efficient algorithms to optimize the BD-RIS with the dynamic grouping strategy.

### III. DYNAMICALLY GROUP-CONNECTED BD-RIS DESIGN

#### A. BD-RIS-Aided MU-MISO with Dynamic Grouping Strategy

To demonstrate the advantage of the proposed CW-DGC architecture, we apply the CW-DGC BD-RIS with the hybrid mode into a MU-MISO system as shown in Fig. 2, where an  $N$ -antenna transmitter serves  $K$  single-antenna users with the assistance of an  $M$ -cell BD-RIS. Among  $K$  users,  $K_r$  users, namely reflective users,  $\mathcal{K}_r = \{1, \dots, K_r\}$ , are located at one side of the BD-RIS, and  $K_t = K - K_r$  users, namely transmissive users,  $\mathcal{K}_t = \{K_r + 1, \dots, K\}$ , are located at the other side,  $\mathcal{K} = \mathcal{K}_t \cup \mathcal{K}_r$ . Define  $\mathbf{s} \triangleq [s_1, \dots, s_K]^T \in \mathbb{C}^K$  as the transmit symbol vector,  $\mathbb{E}\{\mathbf{s}\mathbf{s}^H\} = \mathbf{I}_K$ , and  $\mathbf{W} \triangleq [\mathbf{w}_1, \dots, \mathbf{w}_K] \in \mathbb{C}^{N \times K}$  as the transmit precoder. The received signal at the user side is

$$y_k = \tilde{\mathbf{h}}_k \mathbf{w}_k s_k + \tilde{\mathbf{h}}_k \sum_{p \in \mathcal{K}, p \neq k} \mathbf{w}_p s_p + n_k, \forall k \in \mathcal{K}, \quad (6)$$

where  $\tilde{\mathbf{h}}_k = \mathbf{h}_k^H \Phi_i \mathbf{G}$ ,  $\forall k \in \mathcal{K}_i$ ,  $\forall i \in \{t, r\}$ ,  $\mathbf{h}_k \in \mathbb{C}^M$ ,  $\forall k \in \mathcal{K}$  is the channel vector between the RIS and each user,  $\mathbf{G} \in \mathbb{C}^{M \times N}$  is the channel matrix between the BS and the RIS, and  $n_k \sim \mathcal{CN}(0, \sigma_k^2)$ ,  $\forall k \in \mathcal{K}$  is the noise.

Aiming at jointly optimizing the precoder and BD-RIS matrix to maximize the sum-rate, we have

$$\max_{\mathbf{W}, \Phi_t, \Phi_r} \sum_{k \in \mathcal{K}} \log_2 \left( 1 + \frac{|\tilde{\mathbf{h}}_k^H \mathbf{w}_k|^2}{\sum_{p \in \mathcal{K}, p \neq k} |\tilde{\mathbf{h}}_k^H \mathbf{w}_p|^2 + \sigma_k^2} \right) \quad (7a)$$

$$\text{s.t. } \mathcal{D}_p \cap \mathcal{D}_q = \emptyset, \forall p \neq q, \quad (7b)$$

$$\mathcal{D}_g \neq \emptyset, \forall g, \quad (7c)$$

$$\bigcup_{g=1}^G \mathcal{D}_g = \mathcal{M}, \quad (7d)$$

$$[\Phi_t]_{m,n} = 0, \forall m \in \mathcal{D}_p, \forall n \in \mathcal{D}_q, p \neq q, \quad (7e)$$

$$[\Phi_r]_{m,n} = 0, \forall m \in \mathcal{D}_p, \forall n \in \mathcal{D}_q, p \neq q, \quad (7f)$$

$$\Phi_{t, \mathcal{D}_g}^H \Phi_{t, \mathcal{D}_g} + \Phi_{r, \mathcal{D}_g}^H \Phi_{r, \mathcal{D}_g} = \mathbf{I}_{|\mathcal{D}_g|}, \forall g, \quad (7g)$$

$$\|\mathbf{W}\|_F^2 \leq P, \quad (7h)$$

where  $P$  is the total transmit power at the BS.

#### B. CW-DGC BD-RIS Design

Problem (7) is a joint transmit precoder and BD-RIS design with complicated objective function and constraints. To simplify the design, we first transform problem (7) into a more tractable multi-block problem based on fractional programming by introducing two auxiliary vectors, i.e.,  $\boldsymbol{\nu} \triangleq [\nu_1, \dots, \nu_K]^T \in \mathbb{R}^K$  and  $\boldsymbol{\tau} \triangleq [\tau_1, \dots, \tau_K]^T \in \mathbb{C}^K$ , yielding

$$\max_{\mathbf{W}, \Phi_t, \Phi_r, \boldsymbol{\nu}, \boldsymbol{\tau}} \sum_{k \in \mathcal{K}} \left( \log_2(1 + \nu_k) - \nu_k + 2\Re\{\tilde{\tau}_k^* \tilde{\mathbf{h}}_k^H \mathbf{w}_k\} - \sum_{p \in \mathcal{K}} |\tau_k^* \tilde{\mathbf{h}}_k^H \mathbf{w}_p|^2 + |\tau_k|^2 \sigma_k^2 \right) \quad (8a)$$

$$\text{s.t. } (7b)-(7h), \quad (8b)$$

where  $\tilde{\tau}_k = \sqrt{1 + \nu_k} \tau_k$ ,  $\forall k \in \mathcal{K}$ . Then problem (8) can be efficiently solved by iteratively updating four blocks, i.e.,  $\boldsymbol{\nu}$ ,  $\boldsymbol{\tau}$ ,  $\mathbf{W}$ , and  $\{\Phi_t, \Phi_r\}$ , until convergence. Sub-problems regarding blocks  $\boldsymbol{\nu}$ ,  $\boldsymbol{\tau}$ , and  $\mathbf{W}$  are all convex optimizations whose closed-form solutions can be easily obtained, while the design of block  $\{\Phi_t, \Phi_r\}$  is challenging due to the newly introduced constraints (7b)-(7g). Therefore, in this paper we omit the details for updating the above three blocks due to the space limitation and focus on the design of block  $\{\Phi_t, \Phi_r\}$ .

When  $\mathbf{W}$ ,  $\boldsymbol{\tau}$ , and  $\boldsymbol{\nu}$  are fixed, the first two and the last terms in objective (8a) are constants and can be removed. Therefore, the objective function with respect to  $\Phi_t$  and  $\Phi_r$  is

$$\sum_{k \in \mathcal{K}} \left( \sum_{p \in \mathcal{K}} |\tau_k^* \tilde{\mathbf{h}}_k^H \Phi_i \mathbf{G} \mathbf{w}_p|^2 - 2\Re\{\tilde{\tau}_k^* \tilde{\mathbf{h}}_k^H \Phi_i \underbrace{\mathbf{G} \mathbf{w}_k}_{=\mathbf{g}_k}\} \right) \quad (9a)$$

$$= \sum_{i \in \{t, r\}} \left( \text{Tr}(\Phi_i \underbrace{\sum_{p \in \mathcal{K}} \mathbf{g}_p \mathbf{g}_p^H}_{=\mathbf{Y}} \Phi_i^H \underbrace{\sum_{k \in \mathcal{K}_i} |\tau_k|^2 \mathbf{h}_k \mathbf{h}_k^H}_{=\mathbf{Z}_i}) - 2\Re\{\text{Tr}(\Phi_i \underbrace{\sum_{k \in \mathcal{K}_i} \mathbf{g}_k \mathbf{h}_k^H \tilde{\tau}_k^*}_{=\mathbf{X}_i})\} \right) \quad (9b)$$

$$\stackrel{(a)}{=} \sum_{i \in \{t, r\}} \sum_{g \in \mathcal{G}} \left( \text{Tr}(\Phi_{i, \mathcal{D}_g} \sum_{p \in \mathcal{G}} \mathbf{Y}_{\mathcal{D}_g, \mathcal{D}_p} \Phi_{i, \mathcal{D}_p}^H \mathbf{Z}_{i, \mathcal{D}_p, \mathcal{D}_g}) - 2\Re\{\text{Tr}(\Phi_{i, \mathcal{D}_g} \mathbf{X}_{i, \mathcal{D}_g})\} \right) \quad (9c)$$

$$\approx \sum_{g \in \mathcal{G}} \sum_{i \in \{t, r\}} \left( \text{Tr}(\Phi_{i, \mathcal{D}_g} \mathbf{Y}_{\mathcal{D}_g, \mathcal{D}_g} \Phi_{i, \mathcal{D}_g}^H \mathbf{Z}_{i, \mathcal{D}_g, \mathcal{D}_g}) - 2\Re\{\text{Tr}(\Phi_{i, \mathcal{D}_g} \mathbf{X}_{i, \mathcal{D}_g})\} \right) \quad (9d)$$

$$= \sum_{g \in \mathcal{G}} f_g(\Phi_{t, \mathcal{D}_g}, \Phi_{r, \mathcal{D}_g}) \quad (9e)$$

where (a) holds by defining matrices  $\mathbf{X}_{i, \mathcal{D}_g}$ ,  $\mathbf{Y}_{\mathcal{D}_p, \mathcal{D}_g}$  and  $\mathbf{Z}_{i, \mathcal{D}_p, \mathcal{D}_g}$ ,  $\forall g \in \mathcal{G}$ ,  $\forall i \in \{t, r\}$ , which are sub-matrices selecting rows and columns according to  $\mathcal{D}_g$  from  $\mathbf{X}_i$ , and selecting rows according to  $\mathcal{D}_p$  and columns according to  $\mathcal{D}_g$  from  $\mathbf{Y}$  and  $\mathbf{Z}_i$ ,  $\forall i \in \{t, r\}$ , respectively; (b) holds by the finding (based on large amount of simulations) that the value of the cross term  $\Phi_{i, \mathcal{D}_g} \sum_{p \neq g} \mathbf{Y}_{\mathcal{D}_g, \mathcal{D}_p} \Phi_{i, \mathcal{D}_p}^H \mathbf{Z}_{i, \mathcal{D}_p, \mathcal{D}_g}$  is negligible compared to  $\Phi_{i, \mathcal{D}_g} \mathbf{X}_{i, \mathcal{D}_g}$  due to the severe double fading of the cascaded transmitter-RIS-user channels. Based on the above derivations, the sub-problem with respect to  $\Phi_t$  and  $\Phi_r$  is given by

$$\min_{\Phi_{t, \mathcal{D}_g}, \Phi_{r, \mathcal{D}_g}, \forall g \in \mathcal{G}} \sum_{g \in \mathcal{G}} f_g(\Phi_{t, \mathcal{D}_g}, \Phi_{r, \mathcal{D}_g}) \quad (10a)$$

$$\text{s.t. } (7b)-(7g). \quad (10b)$$

Problem (10) is still difficult to solve due to the coupling of grouping  $\mathcal{D}_1, \dots, \mathcal{D}_G$  and non-zero parts of the BD-RIS matrices  $\Phi_{t/r, \mathcal{D}_g}$ ,  $\forall g \in \mathcal{G}$ . To further simplify the design, we propose to iteratively<sup>3</sup> update  $\mathcal{D}_g$ ,  $\forall g \in \mathcal{G}$  and  $\Phi_{t/r, \mathcal{D}_g}$ ,  $\forall g \in \mathcal{G}$ , until the convergence is achieved.

<sup>3</sup>Note that the initialization of BD-RIS matrix is required, that is, both the dynamic grouping and corresponding non-zero elements of the BD-RIS matrix should be initialized. Here we initialize dynamic grouping sets as  $\mathcal{D}_g = \mathcal{G}_g$ ,  $\forall g$  and corresponding non-zeros parts of RIS matrices as random values.

1) *Dynamic Grouping Optimization*: When RIS matrices are fixed, the grouping problem is

$$\min_{\mathcal{D}_g, \forall g \in \mathcal{G}} \sum_{g \in \mathcal{G}} f_g(\Phi_{t, \mathcal{D}_g}, \Phi_{r, \mathcal{D}_g}) \quad (11a)$$

$$\text{s.t.} \quad (7b)-(7d). \quad (11b)$$

We propose a simple yet practical iterative algorithm to solve the grouping problem. Given a proper initialization of  $\mathcal{D}_1, \dots, \mathcal{D}_G$ , we aim to successively determine which group each RIS cell should belong to based on the following steps.

Step 1: For cell  $m$ ,  $\forall m \in \mathcal{M}$ , we first check which group this cell belongs to and tag the exact position as  $g_{\text{tag}}$ . To guarantee each group contains at least one RIS cell, we check the size of  $\mathcal{D}_{g_{\text{tag}}}$ . When  $|\mathcal{D}_{g_{\text{tag}}}| > 1$ , the following Steps 2-4 are executed.

Step 2: We calculate the value of objective (11a), which is marked as  $\bar{f}_{m,g}$ , when cell  $m$  is either in group  $g_{\text{tag}}$ , i.e.,  $g = g_{\text{tag}}$  or moved to other  $G - 1$  groups, i.e.,  $g \neq g_{\text{tag}}$ , according to (12):

$$\bar{f}_{m,g} = \begin{cases} \sum_{p \in \mathcal{G}} f_p(\Phi_{t, \mathcal{D}_p}, \Phi_{r, \mathcal{D}_p}), & g = g_{\text{tag}}, \\ f_{g_{\text{tag}}}(\Phi_{t, \tilde{\mathcal{D}}_{g_{\text{tag}}}^m}, \Phi_{r, \tilde{\mathcal{D}}_{g_{\text{tag}}}^m}) \\ + f_g(\Phi_{t, \hat{\mathcal{D}}_g^m}, \Phi_{r, \hat{\mathcal{D}}_g^m}) \\ + \sum_{\substack{p \in \mathcal{G} \\ p \neq g \\ p \neq g_{\text{tag}}}} f_p(\Phi_{t, \mathcal{D}_p}, \Phi_{r, \mathcal{D}_p}), & g \neq g_{\text{tag}}, \end{cases} \quad (12)$$

where  $\tilde{\mathcal{D}}_{g_{\text{tag}}}^m = \tilde{\mathcal{D}}_{g_{\text{tag}}} \setminus \{m\}$ ,  $\hat{\mathcal{D}}_g^m = \mathcal{D}_g \cup \{m\}$ .

Step 3: Among all  $\bar{f}_{m,g}$ ,  $\forall g \in \mathcal{G}$ , we find the index with the minimum value, i.e.,

$$g_m^* = \arg \min_g \bar{f}_{m,g}. \quad (13)$$

Step 4: When  $g_m^* \neq g_{\text{tag}}$ , we update the corresponding dynamic subsets as

$$\begin{aligned} \mathcal{D}_{g_m^*} &= \mathcal{D}_{g_m^*} \cup \{m\}, \\ \mathcal{D}_{g_{\text{tag}}} &= \mathcal{D}_{g_{\text{tag}}} \setminus \{m\}. \end{aligned} \quad (14)$$

Successively updating positions of all  $M$  RIS cells, we can obtain the dynamic grouping subsets  $\mathcal{D}_1, \dots, \mathcal{D}_G$ .

2) *BD-RIS Matrix Optimization*: With fixed grouping subsets, the BD-RIS matrix design problem is given by

$$\min_{\Phi_{t, \mathcal{D}_g}, \Phi_{r, \mathcal{D}_g}} f_g(\Phi_{t, \mathcal{D}_g}, \Phi_{r, \mathcal{D}_g}) \quad (15a)$$

$$\text{s.t.} \quad (7g). \quad (15b)$$

With definitions  $\Phi_{\mathcal{D}_g} \triangleq [\Phi_{t, \mathcal{D}_g}^H, \Phi_{r, \mathcal{D}_g}^H]^H \in \mathbb{C}^{2|\mathcal{D}_g| \times |\mathcal{D}_g|}$ ,  $\mathbf{X}_{\mathcal{D}_g} \triangleq [\mathbf{X}_{t, \mathcal{D}_g}, \mathbf{X}_{r, \mathcal{D}_g}] \in \mathbb{C}^{|\mathcal{D}_g| \times 2|\mathcal{D}_g|}$ , and  $\mathbf{Z}_{\mathcal{D}_g} \triangleq \text{blkdiag}(\mathbf{Z}_{t, \mathcal{D}_g, \mathcal{D}_g}, \mathbf{Z}_{r, \mathcal{D}_g, \mathcal{D}_g}) \in \mathbb{C}^{2|\mathcal{D}_g| \times 2|\mathcal{D}_g|}$ , problem (15) can be rewritten as

$$\min_{\Phi_{\mathcal{D}_g}} \text{Tr}(\Phi_{\mathcal{D}_g} \mathbf{Y}_{\mathcal{D}_g, \mathcal{D}_g} \Phi_{\mathcal{D}_g}^H \mathbf{Z}_{\mathcal{D}_g}) - 2\Re\{\text{Tr}(\Phi_{\mathcal{D}_g} \mathbf{X}_{\mathcal{D}_g})\} \quad (16a)$$

$$\text{s.t.} \quad \Phi_{\mathcal{D}_g}^H \Phi_{\mathcal{D}_g} = \mathbf{I}_{|\mathcal{D}_g|}, \quad (16b)$$

which is an unconstrained optimization on the Stiefel manifold and can be solved by typical conjugate-gradient methods on

---

### Algorithm 1 CW-DGC BD-RIS Design

---

**Input:**  $\mathbf{h}_{i,k}, \forall i \in \{t, r\}, \forall k \in \mathcal{K}_i, \mathbf{G}, \boldsymbol{\ell}, \boldsymbol{\tau}, \mathbf{W}, \Phi_t, \Phi_r, \mathcal{D}_1, \dots, \mathcal{D}_G$ .

**Output:**  $\Phi_t^*, \Phi_r^*$ .

```

1: Calculate  $\mathbf{X}_{t/r}, \mathbf{Y}, \mathbf{Z}_{t/r}$ .
2: while no convergence of objective (9e) do
3:   for  $m = 1 : M$  do
4:     Find  $m \in \mathcal{D}_g$  and set  $g_{\text{tag}} = g$ .
5:     if  $|\mathcal{D}_g| > 1$  then
6:       Calculate  $\bar{f}_{m,g}, \forall g$  by (12).
7:       Find  $g_m^*$  by solving  $g_m^* = \arg \min_g \bar{f}_{m,g}$ .
8:       if  $g_m^* \neq g_{\text{tag}}$  then
9:         Update  $\mathcal{D}_{g_m^*} = \mathcal{D}_{g_m^*} \cup \{m\}$ .
10:        Update  $\mathcal{D}_{g_{\text{tag}}} = \mathcal{D}_{g_{\text{tag}}} \setminus \{m\}$ .
11:       end if
12:     end if
13:   end for
14:   Set  $\Phi_t = \mathbf{0}, \Phi_r = \mathbf{0}$ .
15:   for  $g = 1 : G$  do
16:     Split  $\mathbf{X}_{\mathcal{D}_g}, \mathbf{Y}_{\mathcal{D}_g, \mathcal{D}_g}, \mathbf{Z}_{\mathcal{D}_g}$ .
17:     Solve problem (16) by the manifold method [10].
18:     Obtain  $\Phi_{t, \mathcal{D}_g}^*$  and  $\Phi_{r, \mathcal{D}_g}^*$  by (17).
19:     Restore  $\Phi_t^*$  and  $\Phi_r^*$  by (18).
20:   end for
21: end while
22: Return  $\Phi_{t/r}^*$ .
```

---

the manifold space [10]. After solving (16), BD-RIS matrices for each group are

$$\begin{aligned} \Phi_{t, \mathcal{D}_g}^* &= [\Phi_{\mathcal{D}_g}^*]_{1:|\mathcal{D}_g^*|, :}, \forall g \in \mathcal{G} \\ \Phi_{r, \mathcal{D}_g}^* &= [\Phi_{\mathcal{D}_g}^*]_{|\mathcal{D}_g^*|+1:2|\mathcal{D}_g^*|, :}, \forall g \in \mathcal{G}. \end{aligned} \quad (17)$$

With  $\Phi_{t, \mathcal{D}_g}^*$  and  $\Phi_{r, \mathcal{D}_g}^*$ ,  $\forall g \in \mathcal{G}$ , we need to perform a restoring operation to get the original  $\Phi_t^*$  and  $\Phi_r^*$  satisfying (7e) and (7f). To this end, we introduce  $G$  vectors  $\mathbf{d}_g \in \mathbb{R}^{|\mathcal{D}_g|}$ ,  $\forall g \in \mathcal{G}$ , which list the indexes in  $\mathcal{D}_g$  in ascending order. Then we have

$$\begin{aligned} [\Phi_t^*]_{\mathbf{d}_g^T, \mathbf{d}_g^T} &= \Phi_{t, \mathcal{D}_g}^*, \forall g \in \mathcal{G}, \\ [\Phi_r^*]_{\mathbf{d}_g^T, \mathbf{d}_g^T} &= \Phi_{r, \mathcal{D}_g}^*, \forall g \in \mathcal{G}. \end{aligned} \quad (18)$$

3) *Summary*: After iteratively updating grouping subsets and BD-RIS matrices until some convergence thresholds are achieved, we can get  $\mathcal{D}_1^*, \dots, \mathcal{D}_G^*$  and corresponding BD-RIS matrices. For clarity, this CW-DGC BD-RIS design algorithm is summarized in Algorithm 1. The complexity of Algorithm 1 mainly comes from the design of BD-RIS matrix, i.e., lines 14-19 in Algorithm 1, which requires  $\mathcal{O}\{\sum_{g=1}^G I_{\text{cg},g} |\mathcal{D}_g|^3\}$ , where  $I_{\text{cg},g}, \forall g \in \mathcal{G}$ , denotes the number of iterations of the manifold algorithm [10]. Therefore, the complexity of Algorithm 1 is  $\mathcal{O}\{I \sum_{g=1}^G I_{\text{cg},g} |\mathcal{D}_g|^3\}$ , where  $I$  denotes the number of iterations of Algorithm 1.

## IV. PERFORMANCE EVALUATION

In this section, we present simulation results to demonstrate the performance of the proposed design. Simulation settings are summarized in Table I.



TABLE I  
SIMULATION SETTINGS

Parameters	Value	
Channel Model	BS-RIS link	Rician fading ( $\kappa = 3$ dB)
	RIS-user link	Rayleigh fading (i.i.d.)
Signal attenuation	$\zeta_0 = -30$ dB (1 meter)	
Path loss exponent	$\varepsilon = 2.2$	
Noise power	$\sigma_k^2 = -80$ dBm, $\forall k \in \mathcal{K}$	
Distance	BS-RIS link	$d_{\text{BI}} = 50$ m
	RIS-user link	$d_{\text{TU}} = 2.5$ m

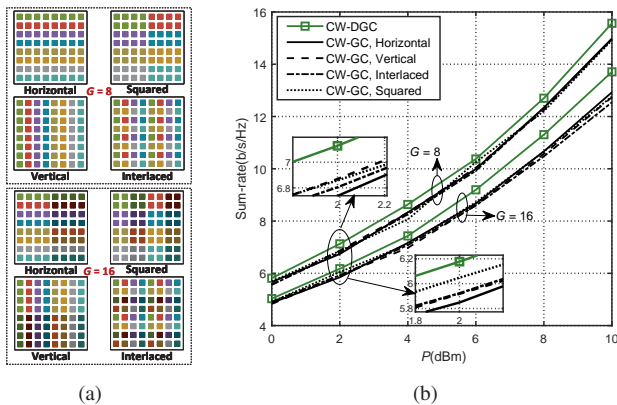


Fig. 4. Comparison among different grouping strategies: (a) Four types of fixed grouping strategies; (b) Sum-rate versus transmit power ( $M = 64$ ,  $N = K = 6$ ,  $K_t = K_r = 3$ ).

Fig. 4 shows a simulation result when BD-RIS has 64 cells ( $8 \times 8$  square). Four fixed grouping strategies, namely “Horizontal”, “Vertical”, “Squared”, “Interlaced”, are used in the simulation as illustrated in 4(a), where cells with the same color belong to the same group. We plot sum-rate performance of different CW-GC schemes in Fig. 4(b). It can be shown that our proposed dynamic grouping strategy outperforms four CW-GC cases. In addition, there are no obvious performance gaps among four CW-GC architectures. Therefore, we can deduce from Fig. 4 that the performance of CW-GC BD-RIS depends more on group size than on locations of cells.

Fig. 5(a) shows the sum-rate versus the number of cells  $M$ . For comparison, we add two baselines, marked as “Cell-Wise Fully-Connected (CW-FC)”, and “Cell-Wise Single-Connected (CW-SC)” [8]. We can observe that with the same number of groups, the “CW-DGC” scheme always achieves a better performance than “CW-GC” scheme<sup>4</sup>. In addition, with a decreasing number of groups, the “CW-DGC” scheme achieves sum-rate performance close to “CW-FC”. Then in Fig. 5(b), we show the sum-rate performance as a function of the number of groups  $G$ . With the growth of the number of groups, equivalently the decrease of the number of non-zero BD-RIS elements, the performance gap between “CW-DGC” and “CW-GC” schemes becomes larger. For example, the performance achieved by “CW-DGC” improves by around 6% when  $G = 16$  while by around 12% with  $G = 32$ . This fact demonstrates that the benefit of dynamic grouping is much more obvious when the size of each group is relatively small.

<sup>4</sup>Given that four fixed grouping strategies have similar performance, in Fig. 5 we only plot the horizontal case, which is marked as “CW-GC”.

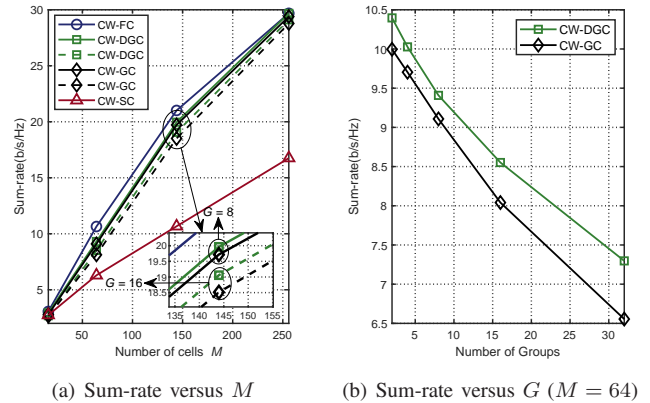


Fig. 5. (a) Sum-rate versus the number of cells  $M$ ; (b) sum-rate versus the number of groups  $G$  ( $N = K = 6$ ,  $K_t = K_r = 3$ ,  $P = 5$  dBm).

## V. CONCLUSIONS

In this paper, we propose a novel CW-DGC architecture for BD-RIS with the hybrid mode. To show the advantage of the proposed architecture, we deploy the CW-DGC BD-RIS into a MU-MISO communication system, and consider the joint dynamic grouping and BD-RIS matrix design to maximize the sum-rate performance. To efficiently solve the problem, we propose a simple yet practical algorithm to iteratively update dynamic grouping and BD-RIS matrix. Finally, simulation results demonstrate that the proposed CW-DGC architecture outperforms fixed CW-GC architectures.

## REFERENCES

- [1] Q. Wu and R. Zhang, “Towards smart and reconfigurable environment: Intelligent reflecting surface aided wireless network,” *IEEE Communications Magazine*, vol. 58, no. 1, pp. 106–112, 2019.
- [2] M. A. ElMossallamy, H. Zhang, L. Song, K. G. Seddik, Z. Han, and G. Y. Li, “Reconfigurable intelligent surfaces for wireless communications: Principles, challenges, and opportunities,” *IEEE Transactions on Cognitive Communications and Networking*, vol. 6, no. 3, pp. 990–1002, 2020.
- [3] S. Shen, B. Clerckx, and R. Murch, “Modeling and architecture design of reconfigurable intelligent surfaces using scattering parameter network analysis,” *IEEE Transactions on Wireless Communications*, vol. 21, no. 2, pp. 1229–1243, 2021.
- [4] M. Nerini and B. Clerckx, “Reconfigurable intelligent surfaces based on single, group, and fully connected discrete-value impedance networks,” *arXiv preprint arXiv:2110.00077*, 2021.
- [5] Q. Li, M. El-Hajjar, I. A. Hemadeh, A. Shojaefard, A. Mourad, B. Clerckx, and L. Hanzo, “Reconfigurable intelligent surfaces relying on non-diagonal phase shift matrices,” *IEEE Transactions on Vehicular Technology*, 2022.
- [6] S. Zhang, H. Zhang, B. Di, Y. Tan, Z. Han, and L. Song, “Beyond intelligent reflecting surfaces: Reflective-transmissive metasurface aided communications for full-dimensional coverage extension,” *IEEE Transactions on Vehicular Technology*, vol. 69, no. 11, pp. 13905–13909, 2020.
- [7] J. Xu, Y. Liu, X. Mu, J. T. Zhou, L. Song, H. V. Poor, and L. Hanzo, “Simultaneously transmitting and reflecting (STAR) intelligent omni-surfaces, their modeling and implementation,” *IEEE Vehicular Technology Magazine*, vol. 17, no. 2, 2022.
- [8] H. Li, S. Shen, and B. Clerckx, “Beyond diagonal reconfigurable intelligent surfaces: From transmitting and reflecting modes to single-, group-, and fully-connected architectures,” *IEEE Transactions on Wireless Communications*, Accepted, 2022.
- [9] —, “Beyond diagonal reconfigurable intelligent surfaces: A multi-sector mode enabling highly directional full-space wireless coverage,” *arXiv preprint arXiv:2209.00301*, 2022.
- [10] P.-A. Absil, R. Mahony, and R. Sepulchre, “Optimization algorithms on matrix manifolds,” in *Optimization Algorithms on Matrix Manifolds*. Princeton University Press, 2009.